Preparation of Activated Carbon from Pyrolyzed Rice Husk by Leaching out Ash Content after CO_2 Activation

Ming Li, Shanwei Ma, and Xifeng Zhu *

To prepare activated carbons with a high porosity and low ash content from pyrolyzed rice husk, the method of KOH or K_2CO_3 solution leaching after CO_2 activation was investigated. The effects of KOH or K_2CO_3 concentration and leaching time on the yield, ash content, and textural properties of the activated carbon were studied, and the activated carbon prepared under the best conditions was characterized. The results showed that the best leaching time was 1 h for KOH and K_2CO_3, and the best concentrations were 1.0 and 4.0 M, respectively. The leaching process was greatly beneficial to the development of the pore structure. The specific surface area of the activated carbon prepared under the most favorable conditions was approximately 1100 m^2/g, and the iodine values were greater than 1100 mg/g. As a result of the leaching process, the ash content of the sample was notably decreased from 63% to approximately 5%, and the porosity development was attributed to the reaction of the leaching reagents with silica.

Keywords: Rice husk; Physical activation; Leaching; Silica; Activated carbon

*Contact information: Key Laboratory for Biomass Clean Energy of Anhui Province, University of Science and Technology of China, Hefei, 230026, China; *Corresponding author: xfzhu@ustc.edu.cn*

INTRODUCTION

Activated carbon is widely used as an adsorbent, catalyst, catalyst supporter, and electrode material (Lillo-Rodenas *et al*. 2003; Olivares-Marin *et al*. 2007), and it plays an important role in wastewater treatment, gas storage, food processing, and the pharmaceutical and chemical industries. However, its high cost limits its applications in most cases (Ozdemir *et al*. 2011). This fact has prompted a growing interest in the production of activated carbon from low-cost precursors. Because of its renewability, low cost, and abundant availability, biomass materials, such as bamboo (Ip *et al*. 2008), cherry stone (Olivares-Marin *et al*. 2012), coconut shell (Li *et al*. 2008), corn cob (Song *et al*. 2013), and rice husk (Zhang *et al*. 2011) have attracted considerable attention recently.

Generally, physical activation and chemical activation are two common methods for the production of activated carbon. Physical activation is usually achieved in two steps: the carbonization of the raw materials at high temperature, and the activation of the carbonized sample with activating gases, such as steam, air, and CO_2. Chemical activation involves the impregnation of the raw materials with a chemical activation agent, such as phosphoric acid (H_3PO_4), hydroxide (NaOH or KOH), carbonate (Na_2CO_3 or K_2CO_3), and zinc chloride ($ZnCl_2$), as well as the activation of the mixture in an inert atmosphere. Compared with the activated carbon prepared by physical activation, samples prepared *via* chemical activation have a larger specific surface area. However, chemical activation is a time-consuming and technically complicated procedure because of the impregnation and drying processes (Basta *et al*. 2009; Liou and Wu 2009). Additionally, equipment corrosion

is a serious problem, and energy consumption is high in the activation process, considering the sample is impregnated with acidic or alkali agents, and is usually activated at temperatures as high as 400 to 900 °C (Guo *et al*. 2002; Olivares-Marin *et al*. 2006; Guo and Rockstraw 2007; Kalderis *et al*. 2008; Ould-Idriss *et al*. 2011).

Rice husk is the major by-product of the rice milling industry, and its annual production in China is over 36 million tons (Zhang *et al*. 2011). Nowadays, rice husk has been widely used as a precursor to prepare porous carbon by physical and chemical activation, and the specific surface area of the prepared activated carbon was in the range of 450 to 2000 m^2/g (Yalcin and Sevinc 2000; Guo and Rockstraw 2007; Ding *et al*. 2014). Besides, rice husk has also been used to produce bio-oil by fast pyrolysis, which is an efficient process to convert biomass into bio-oil, while yielding some non-condensable gases and 15% to 30% solid char byproduct. However, as one of the most promising technologies to massively utilize biomass, poor economy has limited its further development and application. The effective and high-value use of the solid char can significantly improve the economy of bio-oil. Because the pyrolysis temperature is usually in the range of 400 to 550 °C (Chang *et al*. 2012), activated carbon can be produced from the solid char directly by physical activation, and thus lowering the preparation cost because of the absence of the preliminary carbonization stage. However, in the pyrolysis of rice husk, the solid byproduct pyrolyzed rice husk (PR) is rich in ash content, as high as approximately 35% (Li *et al*. 2014), which will prevent porosity evolution by blocking or filling some pores during the activation process (Yun *et al*. 2003; Suzuki *et al*. 2007); therefore, the surface area is usually low for the activated carbon prepared from rice husk by physical activation. Presently, the most common method used to remove ash in the activation of rice husk precursor is by chemical activation using NaOH or KOH as an activating agent (Yeletsky et al. 2009; Xiao *et al*. 2014). The preparation of activated carbon from PR by physical activation following KOH or K_2CO_3 solution leaching has not been well studied (Ding *et al*. 2014). This method presents two main advantages: one is relatively weak corrosion because the leaching process with KOH or K_2CO_3 solution is carried out at 100 °C under atmospheric pressure, and the other is larger porosity of the resulting activated carbon because the most of ash content will be removed in the leaching process. It is worth noting that the physical activation of PR to preliminarily develop pore structure is necessary because the pore structure of PR is less-developed, and its specific surface area is only 5 m^2/g.

The primary objective of this study is to prepare a highly porous activated carbon from PR by leaching out the ash content with KOH or K_2CO_3 after CO_2 activation. The effects of leaching time and KOH or K_2CO_3 concentration on the yield, ash content, and porosity of the activated carbons were investigated. Additionally, the activated carbons prepared under the best conditions were characterized, and their iodine number was measured.

EXPERIMENTAL

Materials

Pyrolyzed rice husk was the byproduct of fast-pyrolyzing rice husk for bio-oil in our laboratory. The variety of rice was *Oryza sativa* ssp. *indica*. The rice was grown in the suburb of Hefei in China, and was harvested and milled in August of 2014. Prior to pyrolysis, the rice husks were ground and sieved to the maximum particle size of 1 mm.

The pyrolysis conditions of rice husk were as follows: 480 °C/s of heating rate, 510 °C of pyrolysis temperature, and 4 s of solid phase residence time. The proximate analysis (dry basis) of PR was previously reported, and the ash, volatile and fixed carbon of PR were 36.1%, 10.5% and 53.4%, respectively (Li *et al*. 2014). The KOH and K_2CO_3 reagents were analytical grade and purchased from Sinopharm Chemical Reagent Co., Ltd., in Shanghai, China.

Preparation of the Activated Carbons

Activated carbon was prepared using two sequential steps: activation and leaching with KOH or K_2CO_3. In the activation process, PR was loaded into a quartz boat, and was placed inside a tube furnace, heated to 900 °C at a rate of 10 °C/min under N_2 (500 cm^3/min). Then, the gas supply was adjusted from N_2 to CO_2 (800 cm^3/min), and PR was activated for 1 h. Finally, the sample was cooled to room temperature under a N_2 atmosphere (500 cm^3/min). The obtained sample was denoted as APR, and the yield of APR was 53.9%. For the leaching process, 5.0 g of APR was refluxed with a set concentration of KOH or K_2CO_3 solution (50 cm^3) in a glass round-bottomed flask at 100 °C oil bath for 0.5 to 4 h. Then, the mixture was filtrated, and the precipitate was washed repeatedly with hot distilled water until a neutral pH was obtained. Following filtration, the sample was dried at 110 °C for 24 h to obtain the final product. All of the experiments were repeated three times, and the relative standard deviation was less than 3%.

Characterization of the Activated Carbons

The specific surface area and pore structure characteristics of the prepared activated carbon were determined by nitrogen adsorption at −196 °C (Quadrasorb SI, Quantachrome Instruments, USA). Prior to the gas adsorption measurement, the sample was degassed under a N_2 atmosphere at 150 °C for 5 h. The specific surface area (S_{BET}) was calculated according to the Brunauer–Emmett–Teller (BET) equation at a relative pressure p/p_0 of 0.05 to 0.2. The total pore volume (V_t) was estimated to be the liquid volume of the adsorbate (N_2) at a relative pressure p/p_0 of 0.985 (Yang and Lua 2003). The t-plot method was used to calculate the micropore volume (V_{micro}). The mesopore volume (V_{meso}) was determined by subtracting the micropore volume from the total pore volume, while the mesopore percentage (η) was based on the total pore volume (Yang and Qiu 2011). The pore size distribution was calculated from the N_2 adsorption isotherm, using the Berret–Joyner–Halenda (BJH) method. The average pore diameter (D) was calculated using the equation: $D = 4000V/S_{BET}$ (Song *et al*. 2012).

To learn about the evolution of crystallites of carbon and silica in the preparation of activated carbon, the X-ray diffraction (XRD) pattern analysis was performed on a powder XRD analyzer (MXPAHF, MacScience Co., Japan). The morphology was characterized by a scanning electron microscope (SEM; Sirion200, FEI Quanta, USA). The framework vibration was examined to qualitatively investigate the surface functional groups by a Fourier transform infrared spectrometer (FTIR; Nicolet 6700, Thermo Scientific, USA). The yield η (%) of the prepared activated carbon in the leaching process was calculated *via* the mass ratio of the resulting activated carbon to APR. The ash content was determined according to the ASTM D2866 (1994) testing standard, and it was the ratio of the ash mass to the mass of the measured sample. The ash component was determined by an X-ray fluorescence analyzer (XRF; XRF–1800, Shimadzu, Japan), and before measurement, the sample was burned to ash according to the method to determine the ash

content. The iodine number was measured according to the ASTM D4607 (1986) testing standard.

In order to investigate the mechanism of the porosity development in the leaching process, the mass reduction and ash mass reduction of per unit mass APR in the leaching process were defined as the mass reduction ratio Δm (%) and the ash mass reduction ratio Δm_{ash} (%), and calculated as follows: $\Delta m = (1 - \eta) \times 100\%$ and $\Delta m_{ash} = (A_0 - \eta \times A) \times 100\%$, respectively, where η (%) is the yield of the prepared activated carbon in the leaching process, A_0 (%), a constant of 63.13%, is the ash content of APR, and A (%) is the ash content of the prepared activated carbon.

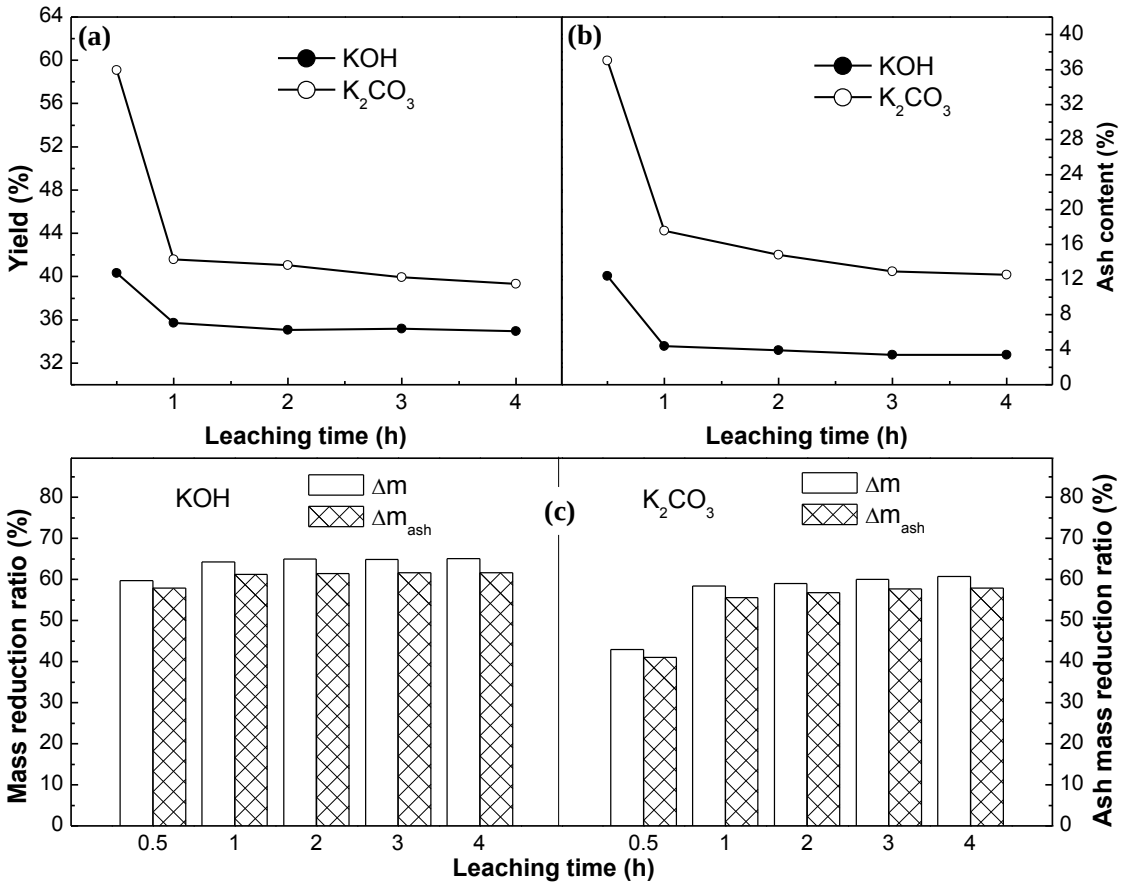

Fig. 1. Effects of leaching time on (a) the yield and (b) the ash content of the activated carbon, and (c) the mass reduction ratio and the ash mass reduction ratio of APR in the leaching process (KOH and K_2CO_3 concentration 3.0 M)

RESULTS AND DISCUSSION

Effects of Leaching Time

To investigate the effects of leaching time on the yield and textural properties of the activated carbons, APR was leached with 3.0 M KOH or K_2CO_3 for 0.5, 1, 2, 3, and 4 h, respectively. As can be seen from Fig. 1(a), a considerable decrease of the yield was observed with increasing leaching time from 0.5 h to 1 h, whereas a further increment from 1 h to 4 h resulted in only slight variations. In addition, under the same leaching time, the yield of the activated carbon leached by KOH was smaller than that of the activated carbon

leached by K_2CO_3. For example, the yields of the activated carbon leached using KOH and K_2CO_3 for 1 h were 35.73% and 41.60%, respectively. It can be observed from Fig. 1(b) that the ash content of the activated carbon showed the same curves as the yield. The ash content decreased from 63.13% to 17.59% and 4.43% in the leaching process for 1 h for KOH and K_2CO_3, respectively. The mass reduction ratio and the ash mass reduction ratio of APR in the leaching process are shown in Fig. 1(c). It can be seen that the mass reduction ratio was slightly larger than the ash mass reduction ratio, and the absolute error was less than 3.5%. This was because small amount of sample was adhered to the filter paper and lost in the wash cycle, so the mass reduction ratio was virtually identical to the ash mass reduction ratio, which means the weight loss of APR in the leaching process was mainly a result of the removal of the ash content.

Table 1 shows the textural properties of APR and the activated carbon obtained by KOH or K_2CO_3 leaching for different time periods. It can be seen that the leaching process was greatly beneficial in improving the specific surface area and pore volume of the activated carbon. The increase of the specific surface area and pore volume with the increase of the leaching time showed similar trends as the decrease of the yield and ash content. The specific surface area increased considerably, from 389 m^2/g to 1131 m^2/g and 972 m^2/g after APR was leached for 1 h with KOH or K_2CO_3, respectively. However, when the leaching time was extended to 2 h or more, the specific surface area and pore volume remained roughly constant. It can also be seen from Table 1, that the micropore and mesopore volume were simultaneously increased as a result of the leaching process, which indicated that the opening of previously inaccessible pores, the creation of new pores, and the widening of the existing pores, happened simultaneously (Daud *et al*. 2000). On the other hand, the mesopore percentages increased from 43.4% to 60.0% and 63.7% for KOH and K_2CO_3 leached samples for 0.5 h, respectively, and then they decreased slightly, to 58% and 61%, with a further increase in the leaching time. The average pore size showed the same trend as the mesopore percentage. This was expected, as the massive external silica reacted with the leaching reagents initially (Suzuki *et al*. 2007; Zhang *et al*. 2014); therefore, the walls of the newly generated pores were destroyed and more mesopores were developed. Consequently, small amounts of previously inaccessible silica were exposed, following the formation of masses of pores, and reacted with the leaching reagents, so that more micropores were generated in this stage.

Table 1. Effects of Leaching Time on Textural Properties of the Activated Carbon

	Leaching time (h)	S_{BET} (m^2/g)	V_t (cm^3/g)	V_{micro} (cm^3/g)	V_{meso} (cm^3/g)	η (%)	D (nm)
KOH	0[a]	389	0.255	0.144	0.111	43.4	2.61
	0.5	1001	0.759	0.304	0.455	60.0	3.03
	1	1131	0.849	0.347	0.502	59.1	3.00
	2	1149	0.873	0.371	0.502	57.5	3.04
	3	1125	0.839	0.347	0.492	58.7	2.98
	4	1132	0.854	0.362	0.492	57.6	3.02
K_2CO_3	0.5	728	0.606	0.220	0.386	63.7	3.33
	1	972	0.741	0.286	0.455	61.4	3.05
	2	1014	0.768	0.298	0.470	61.2	3.03
	3	1030	0.772	0.297	0.475	61.5	3.00
	4	1029	0.787	0.300	0.487	61.9	3.06

[a] APR

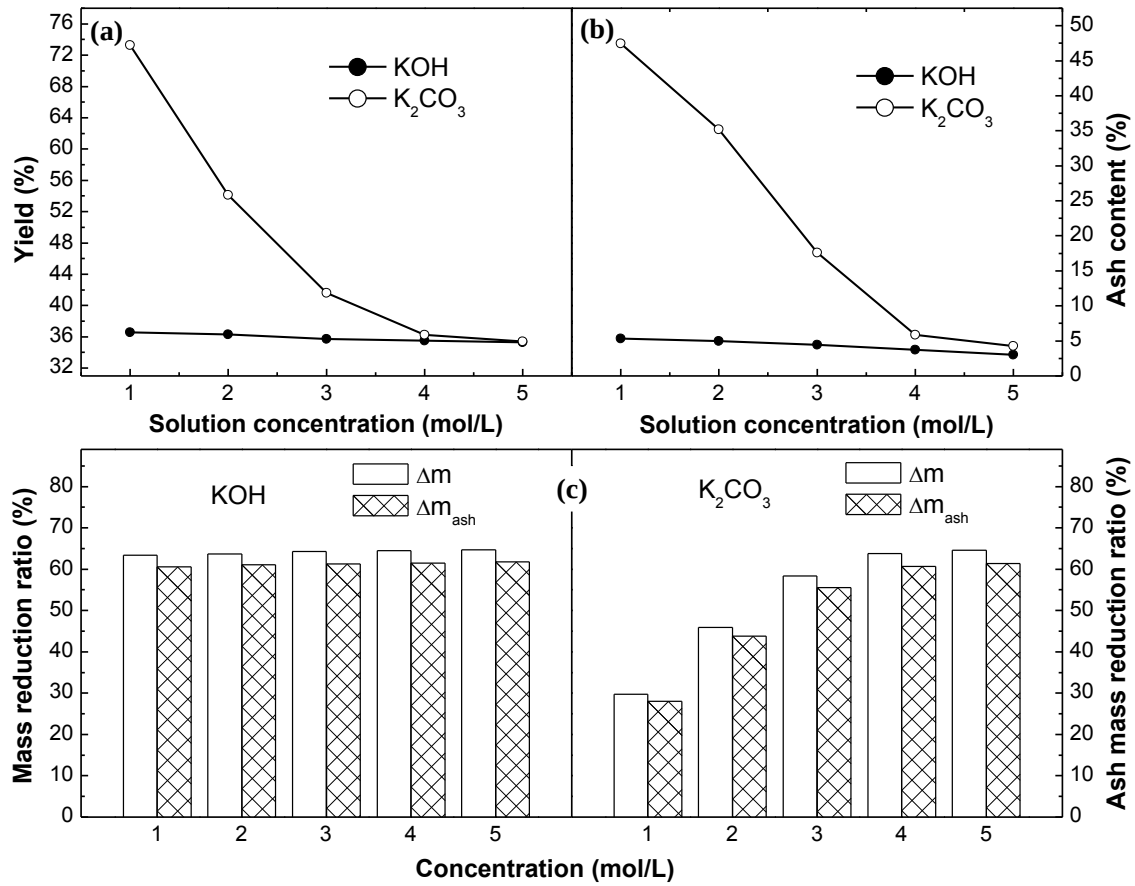

Fig. 2. Effects of solution concentration on (a) the yield and (b) ash content of the activated carbon, and (c) the mass reduction ratio and the ash mass reduction ratio of APR in the leaching process (leaching time 1 h)

On the basis of the results of the yield and textural properties, the best leaching time was judged to be 1 h, and this time period was used for the subsequent experiments.

Effects of KOH and K_2CO_3 Concentration

In this part of the study, different concentrations of KOH and K_2CO_3 solutions (1.0 to 5.0 M) were used to prepare activated carbons. As shown in Fig. 2(a), the yield of activated carbon showed less variation in the studied KOH concentration range and remained at about 36%, whereas the yield decreased rapidly when the K_2CO_3 concentration was varied from 1.0 to 4.0 M, and then displayed a small decrease with a further increase in the K_2CO_3 concentration. As shown in Fig. 2(b), the ash content with the KOH and K_2CO_3 concentration followed the same trend as the yield, which was in agreement with the effects of leaching time on the yield and ash content. The mass reduction ratio and the ash mass reduction ratio of APR in the leaching process with KOH and K_2CO_3 solution concentration presented in Fig.2(c) shows the same results as discussed in the above section. Table 2 shows the textural properties of the activated carbons obtained by leaching with different KOH and K_2CO_3 concentration solutions. It was observed that the increasing trends in the specific surface area and pore volume were consistent with the decreasing trends of the ash content, which indicates that the development of porosity was a result of the removal of the ash component. Furthermore, it can be concluded that the best KOH and K_2CO_3 concentrations were 1.0 and 4.0 M, respectively. The activated carbon prepared

under the best leaching conditions of KOH and K_2CO_3 were labeled as APR–KOH and APR–K_2CO_3, respectively.

Table 2. Effects of Solution Concentration on the Textural Properties of Activated Carbon

	Concentration (mol/L)	S_{BET} (m^2/g)	V_t (cm^3/g)	V_{micro} (cm^3/g)	V_{meso} (cm^3/g)	η (%)	D (nm)
KOH	1	1093	0.801	0.336	0.465	58.1	2.93
	2	1107	0.834	0.339	0.495	59.4	3.01
	3	1131	0.849	0.347	0.502	59.1	3.00
	4	1138	0.850	0.351	0.499	58.7	2.99
	5	1146	0.851	0.354	0.497	58.4	2.97
K_2CO_3	1	608	0.486	0.171	0.315	64.8	3.20
	2	812	0.655	0.230	0.425	64.8	3.22
	3	972	0.741	0.286	0.455	61.4	3.05
	4	1097	0.828	0.334	0.494	59.7	3.02
	5	1121	0.837	0.343	0.494	59.0	2.99

Table 3 shows the XRF results of APR, APR–KOH, and APR–K_2CO_3. It was observed that the silica content in APR–KOH and APR–K_2CO_3 was reduced to approximately 5%, which is far less than the initial value of 67.03% in APR. It can be calculated from the SiO_2 content and ash content of APR, APR–KOH, and APR–K_2CO_3 and the yield of APR–KOH and APR–K_2CO_3 that the SiO_2 mass was reduced in the leaching process by 99.76% and 99.71% percent for APR–KOH and APR–K_2CO_3, respectively. This shows that silica in APR can largely react with KOH or K_2CO_3 during the leaching process. Three main reactions possibly exist in the KOH or K_2CO_3 leaching process, namely the leaching reagents with carbon and SiO_2, and CO_2 with carbon. However, the reaction of KOH or K_2CO_3 with carbon occurs at around 400 and 700 °C, respectively (Lillo-Rodenas *et al*. 2003; Yeletsky *et al*. 2009); therefore, the weight loss of APR in the leaching process is attributed to the reaction of the leaching reagent with silica, in which water-soluble potassium silicate is formed and then removed by filtration. This can be demonstrated by the K_2O content shown in Table 3. As a result, activated carbon with a well-developed porosity was prepared from physically-activated rice husk char. The specific surface areas of APR–KOH and APR–K_2CO_3 were around 1100 m^2/g, and favorably comparable to that of typical commercial activated carbon, which was usually in the range of 400 to 1500 m^2/g (Suzuki *et al*. 2007). According to the results of iodine-adsorbing tests, APR–KOH and APR–K_2CO_3 presented good iodine adsorption performance, and their iodine values were 1141 mg/g and 1125 mg/g, respectively.

Table 3. XRF Results for APR, APR–KOH, and APR–K_2CO_3

Sample	Components (%)								
	SiO_2	K_2O	Na_2O	Fe_2O_3	CaO	MgO	P_2O_5	Al_2O_3	MnO
APR	67.03	1.28	0.11	0.14	0.37	0.17	0.38	0.01	0.15
APR-KOH	5.18	0.10	0.12	0.16	1.05	0.55	0.60	0.03	0.28
APR-K_2CO_3	5.44	0.13	0.12	0.37	0.94	0.50	0.51	0.05	0.29

Characterization Results

Figure 3 shows the nitrogen adsorption and desorption isotherms and the pore size distribution curves of APR–KOH and APR–K_2CO_3. According to the International Union of Pure and Applied Chemistry (IUPAC 1985) classification, the isotherms are of a mixture of type I and IV, because they display sharp knees at relative pressures below 0.1, which is attributed to the presence of micropores (Yeletsky *et al*. 2009). At relative pressure above 0.4, hysteresis loops can be observed, suggesting the presence of mesopores. The pore size distribution of APR–KOH and APR–K_2CO_3 show peak at above 2 nm, and this also confirms that APR–KOH and APR–K_2CO_3 contained mesopores.

The XRD patterns of PR, APR, APR–KOH, and APR–K_2CO_3 are shown in Fig. 4. As seen from the patterns of PR and APR, the peak at around 22° is ascribed to amorphous silica (Song *et al*. 2012). The peak at about 44° of APR is assigned to the (100) plane, indicating the localized graphitization of the structure (Wang *et al*. 2011). This is because of the decrease in the nonparallel single layers and some edge orientation in the CO_2 activation (Wang *et al*. 2009). The diffraction patterns of APR–KOH and APR–K_2CO_3 show a broad peak at about 24°, which is ascribed to the overlap of the silica characteristic peak at about 22° because of the slight silica residue (about 5% as shown in Table 3) and the (002) plane peak at 26° (Kennedy *et al*. 2004; Song *et al*. 2012).

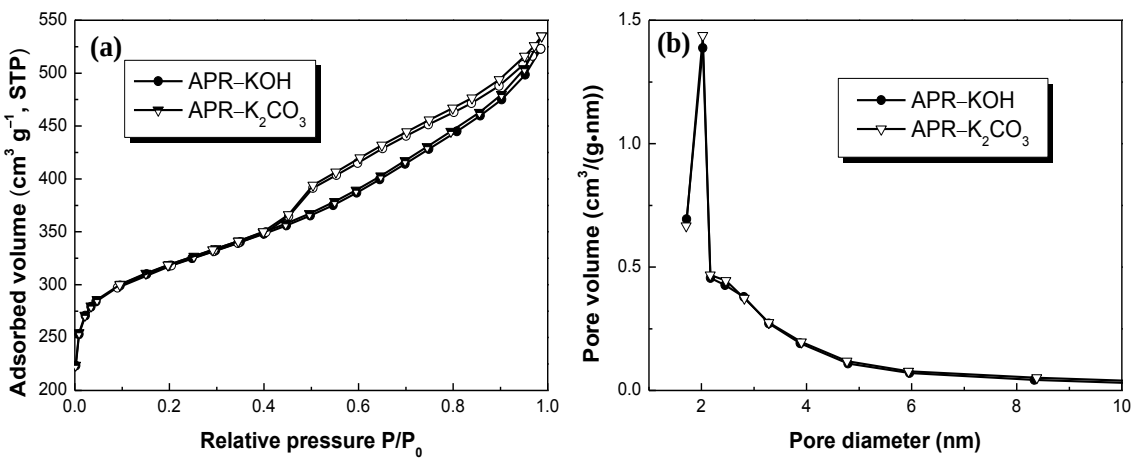

Fig. 3. (a) The nitrogen adsorption–desorption isotherms and (b) the pore size distribution of APR–KOH and APR–K_2CO_3

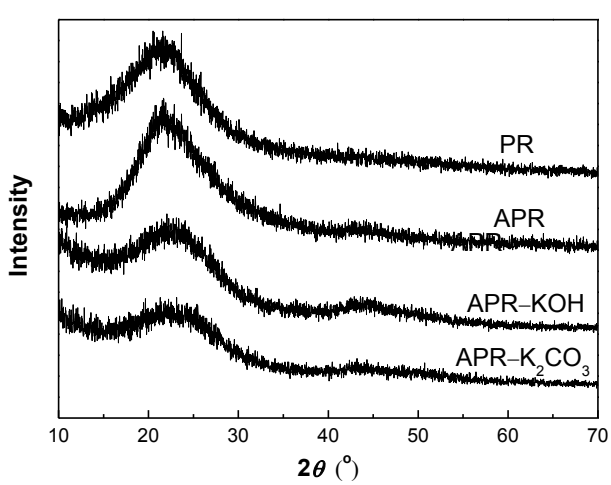

Fig. 4. The XRD patterns of PR, APR, APR–KOH, and APR–K_2CO_3

The FTIR spectra of PR, APR, APR–KOH, and APR–K_2CO_3 are presented in Fig. 5. The wide band at 3420 cm^{-1} is attributed to the O–H stretching vibration of hydroxyl groups or adsorbed water. The bands observed around 2927 cm^{-1} and 2852 cm^{-1} are attributed to the C–H stretching vibration of $–CH_2$. The small band near 1700 cm^{-1} is ascribed to the C=O stretching vibration of ketones, aldehydes, lactones, or carboxyl groups. The band around 1606 cm^{-1} is ascribed to aromatic ring or C=C stretching vibration, demonstrating the carbonization of the precursor. The bands at 1450 cm^{-1} and 1375 cm^{-1} are assigned to the bending vibration of $–CH_3$. Comparing the spectrum of APR with that of PR, the relative intensity of the O–H vibration decreased, and the C–H vibration of methyl and methylene groups and the C=O vibration disappeared. This was owing to the release of the volatiles and the aromatization of the precursor in the CO_2 activation process. The bands in PR and APR at 1100 cm^{-1}, 800 cm^{-1}, and 470 cm^{-1} were assigned to the stretching vibration of silica (Liou 2004). The absence of the symmetric stretching vibration at 780 cm^{-1} indicated that the silica in the samples was amorphous, which is consistent with the result of XRD. After leaching with KOH or K_2CO_3, the characteristic bands of silica almost disappeared, demonstrating the effective removal of the ash content in the leaching process. Apart from this, the spectra of APR–KOH and APR–K_2CO_3 showed the same profile as that of APR, which further illustrated that there were no other reactions taking place during the leaching process except for the reaction of silica with KOH or K_2CO_3. Additionally, the spectra of APR, APR–KOH, and APR–K_2CO_3 became flatter, which was because of an increased structural symmetry, and as a result, there was no change in the dipole moment when the atoms vibrated, and hence there was less intensity in the infrared absorption (Olivares-Marin *et al*. 2006).

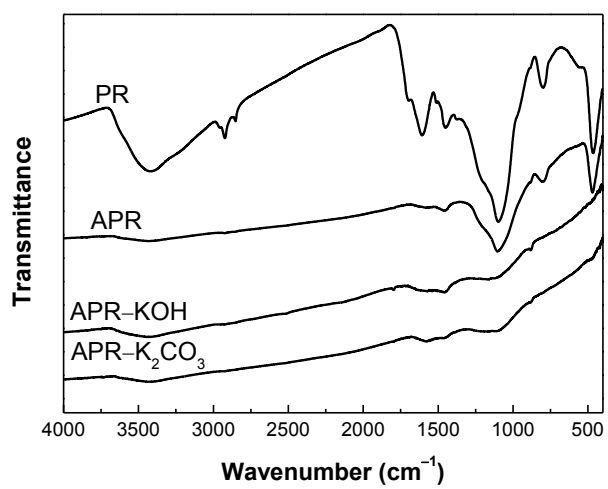

Fig. 5. The FTIR spectra of PR, APR, APR–KOH, and APR–K_2CO_3

The SEM images of PR, APR, APR–KOH, and APR–K_2CO_3 are shown in Fig. 6. As shown in Fig. 6(a), only a few occasional cracks were present on the surface of the particles of PR, which was attributed to the pyrolysis of organic matter. As shown in Fig. 6(b), the sample activated by CO_2 exhibited rudimentary porosity, and some cylinder-shaped pores were clearly identified from the micrograph. As shown in Figs. 6(c) and 6(d), APR was further dissociated into fine particles, and the surface became rougher after leaching with KOH or K_2CO_3, indicating the erosion caused by the reaction of the leaching reagents with silica. The difference between Figs. 6(c) and 6(d) resulted from the different

cross section of particles in the observation. It can be seen that the resultant activated carbon exhibited a well-developed porous structure containing different size pores, which has been confirmed by the textural properties, as summarized in Table 2.

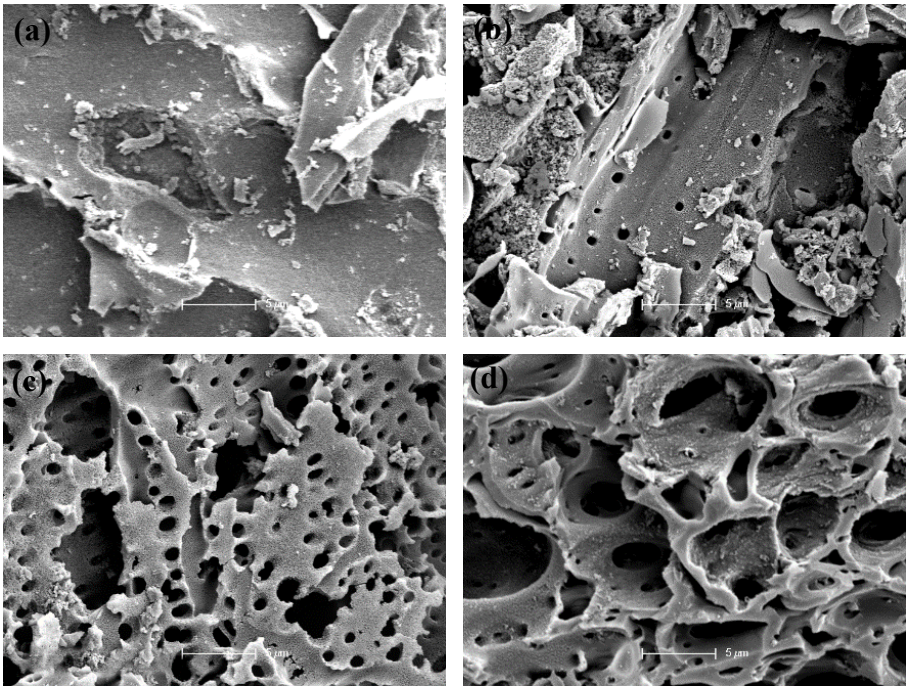

Fig. 6. The SEM images of (a) PR, (b) APR, (c) APR–KOH, and (d) APR–K_2CO_3

CONCLUSIONS

1. Pyrolyzed rice husk is a promising material to prepare activated carbon by KOH or K_2CO_3 leaching after CO_2 activation. For KOH and K_2CO_3, on the basis of the yield, the ash content and the specific surface area, the best leaching time was 1 h, and the best concentration was 1.0 and 4.0 M, respectively. The specific surface areas of the activated carbon prepared under the best conditions were increased from 389 to approximately 1100 m^2/g, with good iodine adsorption performance.
2. In the leaching process, the mass reduction ratio is virtually identical to the ash mass reduction ratio, so the weight loss of sample in the leaching process is mainly a result of the removal of the ash content. The silica mass of the sample under the best leaching conditions was reduced by more than 99% percent, and the porous structure development was mainly attributable to the removal of silica.

ACKNOWLEDGMENTS

The authors acknowledge the financial support provided by the National Basic Research Program of China (2013CB228103) and the Key Research Program of the Chinese Academy of Sciences (KGZD-EW-304-3).

REFERENCES CITED

ASTM D2866 (1994). "Standard test method for total ash content of activated carbon," American Society for Testing and Materials, Philadelphia, USA

ASTM D4607 (1986). "Standard test method for determination of iodine number of activated carbon," American Society for Testing and Materials, Philadelphia, USA

Basta, A. H., Fierro, V., Ei-Saied, H., and Celzard, A. (2009). "2-Steps KOH activation of rice straw: An efficient method for preparing high-performance activated carbons," *Bioresour. Technol.* 100(17), 3941-3947. DOI: 10.1016/j.biortech.2009.02.028

Chang, C. C., Wu, S. R., Lin, C. C., Wan, H. P., and Lee, H. T. (2012). "Fast pyrolysis of biomass in pyrolysis gas: Fractionation of pyrolysis vapors using a spray of bio-oil," *Energy Fuels* 26(5), 2962-2967. DOI: 10.1021/Ef201858h

Daud, W. M. A. W., Ali, W. S. W., and Sulaiman, M. Z. (2000). "The effects of carbonization temperature on pore development in palm-shell-based activated carbon," *Carbon* 38(14), 1925-1932. DOI: 10.1016/S0008-6223(00)00028-2

Ding, L. L., Zou, B., Shen, L., Zhao, C., Wang, Z. C., Guo, Y. P., Wang, X. F., and Liu, Y. H. (2014). "A simple route for consecutive production of activated carbon and liquid compound fertilizer from rice husk," *Colloid Surf. A* 446, 90-96. DOI: 10.1016/j.colsurfa.2014.01.055

Guo, Y. P., and Rockstraw, D. A. (2007). "Activated carbons prepared from rice hull by one-step phosphoric acid activation," *Micropor. Mesopor. Mat.* 100(1-3), 12-19. DOI: 10.1016/j.micromeso.2006.10.006

Guo, Y. P., Yang, S. F., Yu, K. F., Zhao, J. Z., Wang, Z. C., and Xu, H. D. (2002). "The preparation and mechanism studies of rice husk based porous carbon," *Mater. Chem. Phys.* 74(3), 320-323. DOI: 10.1016/S0254-0584(01)00473-4

Ip, A. W. M., Barford, J. P., and Mckay, G. (2008). "Production and comparison of high surface area bamboo derived active carbons," *Bioresour. Technol.* 99(18), 8909-8916. DOI: 10.1016/j.biortech.2008.04.076

Kalderis, D., Bethanis, S., Paraskeva, P., and Diamadopoulos, E. (2008). "Production of activated carbon from bagasse and rice husk by a single-stage chemical activation method at low retention times," *Bioresour. Technol.* 99(15), 6809-6816. DOI: 10.1016/j.biortech.2008.01.041

Kennedy, L. J., Vijaya, J. J., and Sekaran, G. (2004). "Effect of two-stage process on the preparation and characterization of porous carbon composite from rice husk by phosphoric acid activation," *Ind. Eng. Chem. Res.* 43(8), 1832-1838. DOI: 10.1021/Ie034093f

Li, W., Yang, K. B., Peng, J. H., Zhang, L. B., Guo, S. H., and Xia, H. Y. (2008). "Effects of carbonization temperatures on characteristics of porosity in coconut shell chars and activated carbons derived from carbonized coconut shell chars," *Ind. Crop. Prod.* 28(2), 190-198. DOI: 10.1016/j.indcrop.2008.02.012

Li, M., Zheng, Y., Chen, Y. X., and Zhu, X. F. (2014). "Biodiesel production from waste cooking oil using a heterogeneous catalyst from pyrolyzed rice husk," *Bioresour. Technol.* 154, 345-348. DOI: 10.1016/j.biortech.2013.12.070

Lillo-Rodenas, M. A., Cazorla-Amoros, D., and Linares-Solano, A. (2003). "Understanding chemical reactions between carbons and NaOH and KOH - An insight into the chemical activation mechanism," *Carbon* 41(2), 267-275. DOI: 10.1016/S0008-6223(02)00279-8

Liou, T. H. (2004). "Preparation and characterization of nano-structured silica from rice husk," *Mat. Sci. Eng. A-Struct.* 364(1-2), 313-323. DOI: 10.1016/j.msea.2003.08.045

Liou, T. H., and Wu, S. J. (2009). "Characteristics of microporous/mesoporous carbons prepared from rice husk under base- and acid-treated conditions," *J. Hazard. Mater.* 171(1-3), 693-703. DOI: 10.1016/j.jhazmat.2009.06.056

Olivares-Marin, M., Fernandez-Gonzalez, C., Macias-Garcia, A., and Gomez-Serrano, V. (2006). "Preparation of activated carbons from cherry stones by activation with potassium hydroxide," *Appl. Surf. Sci.* 252(17), 5980-5983. DOI: 10.1016/j.apsusc.2005.11.018

Olivares-Marin, M., Fernandez-Gonzalez, C., Macias-Garcia, A., and Gomez-Serrano, V. (2007). "Porous structure of activated carbon prepared from cherry stones by chemical activation with phosphoric acid," *Energy Fuels* 21(5), 2942-2949. DOI: 10.1021/Ef060652u

Olivares-Marin, M., Fernandez-Gonzalez, C., Macias-Garcia, A., and Gomez-Serrano, V. (2012). "Preparation of activated carbon from cherry stones by physical activation in air. Influence of the chemical carbonisation with H_2SO_4," *J. Anal. Appl. Pyrol.* 94, 131-137. DOI: 10.1016/j.jaap.2011.11.019

Ould-Idriss, A., Stitou, M., Cuerda-Correa, E. M., Fernandez-Gonzalez, C., Macias-Garcia, A., Alexandre-Franco, M. F., and Gomez-Serrano, V. (2011). "Preparation of activated carbons from olive-tree wood revisited. I. Chemical activation with H_3PO_4," *Fuel Process. Technol.* 92(2), 261-265. DOI: 10.1016/j.fuproc.2010.05.011

Ozdemir, M., Bolgaz, T., Saka, C., and Sahin, O. (2011). "Preparation and characterization of activated carbon from cotton stalks in a two-stage process," *J. Anal. Appl. Pyrol.* 92(1), 171-175. DOI: 10.1016/j.jaap.2011.05.010

Song, X. L., Zhang, Y., and Chang, C. M. (2012). "Novel method for preparing activated carbons with high specific surface area from rice husk," *Ind. Eng. Chem. Res.* 51(46), 15075-15081. DOI: 10.1021/Ie3012853

Song, M., Jin, B. S., Xiao, R., Yang, L., Wu, Y. M., Zhong, Z. P., and Huang, Y. J. (2013). "The comparison of two activation techniques to prepare activated carbon from corn cob," *Biomass Bioenergy* 48, 250-256. DOI: 10.1016/j.biombioe.2012.11.007

Suzuki, R. M., Andrade, A. D., Sousa, J. C., and Rollemberg, M. C. (2007). "Preparation and characterization of activated carbon from rice bran," *Bioresour. Technol.* 98(10), 1985-1991. DOI: 10.1016/j.biortech.2006.08.001

Wang, H. L., Gao, Q. M., and Hu, J. (2009). "High hydrogen storage capacity of porous carbons prepared by using activated carbon," *J. Am. Chem. Soc.* 131(20), 7016-7022. DOI: 10.1021/Ja8083225

Wang, L. L., Guo, Y. P., Zou, B., Rong, C. G., Ma, X. Y., Qu, Y. N., Li, Y., and Wang, Z. C. (2011). "High surface area porous carbons prepared from hydrochars by phosphoric acid activation," *Bioresour. Technol.* 102(2), 1947-1950. DOI: 10.1016/j.biortech.2010.08.100

Xiao, Y., Chen, H. B., Zheng, M. T., Dong, H. W., Lei, B. F., and Liu, Y. L. (2014). "Porous carbon with ultrahigh specific surface area derived from biomass rice hull," *Mater. Lett.* 116, 185-187. DOI: 10.1016/j.matlet.2013.11.007

Yalcin, N., and Sevinc, V. (2000). "Studies of the surface area and porosity of activated carbons prepared from rice husks," *Carbon*. 38(14), 1943-1945. DOI: 10.1016/S0008-6223(00)00029-4

Yang, T., and Lua, A. C. (2003). "Characteristics of activated carbons prepared from pistachio-nut shells by physical activation," *J. Colloid Interf. Sci.* 267(2), 408-417. DOI: 10.1016/S0021-9797(03)00689-1

Yang, J. A., and Qiu, K. Q. (2011). "Development of high surface area mesoporous activated carbons from herb residues," *Chem. Eng. J.* 167(1), 148-154. DOI: 10.1016/j.cej.2010.12.013

Yeletsky, P. M., Yakovlev, V. A., Mel'gunov, M. S., and Parmon, V. N. (2009). "Synthesis of mesoporous carbons by leaching out natural silica templates of rice husk," *Micropor. Mesopor. Mat.* 121(1-3), 34-40. DOI: 10.1016/j.micromeso.2008.12.025

Yun, C. H., Park, Y. H., Oh, G. H., and Park, C. R. (2003). "Contribution of inorganic components in precursors to porosity evolution in biomass-based porous carbons," *Carbon* 41(10), 2009-2012. DOI: 10.1016/S0008-6223(03)00154-4

Zhang, J. H., Fu, H., Lv, X. S., Tang, J., and Xu, X. H. (2011). "Removal of Cu(II) from aqueous solution using the rice husk carbons prepared by the physical activation process," *Biomass Bioenergy* 35(1), 464-472. DOI: 10.1016/j.biombioe.2010.09.002

Zhang, Y., Zheng, R., Zhao, J. Y., Ma, F., Zhang, Y. C., and Meng, Q. J. (2014). "Characterization of H_3PO_4-treated rice husk adsorbent and adsorption of copper(II) from aqueous solution," *Biomed. Res. Intern*. 2014, 496878. DOI: 10.1155/2014/496878

Article submitted: November 23, 2015; Peer review completed: January 14, 2016; Revised version received and accepted: January 25, 2016; Published: February 18, 2016.
DOI: 10.15376/biores.11.2.3384-3396